

Low Refrigerant Charge Air To Water Domestic Heat Pump Using R-290 As The Refrigerant

van Beek Marcel^(a), van Gorp Thijs^(a)

(a) Re/Gent B.V.

Helmond, 5705BZ, The Netherlands, marcel.van.beek@re-gent.nl

ABSTRACT

The design process and the final design of a demonstration prototype air to water heat pump using a low refrigerant charge of R-290 is described. Component selection is supported by refrigerant charge calculation and experimental investigation using the PVT-superheat method. It is shown that the charge calculations and measurements agree within 6% based on the complete system. The prototype, having a R-290 refrigerant charge of 150 g and built using commercially available components, has a measured nominal heating capacity of 3.4 kW, and a measured system COP of 4.5 at A7/W35 (EN 14511). When combined with an A-label natural gas boiler, in hybrid configuration, A++ efficiency class results ((EU) No 811/2013). Comparison with measurement results of a commercially available hybrid heat pump, shows that the efficiency levels of the prototype correspond with current state of the art systems.

Keywords: Propane, Low Charge, Heat pump, Design, Prototype

1. INTRODUCTION

In the Netherlands domestic dwellings are predominately heated using natural gas fired boilers. Current legislation already prohibits the use of natural gas heating in new built houses and Dutch government policy targets zero domestic use in 2050. Small air to water heat pumps, in hybrid configuration with a natural gas boiler, are seen as the solution for reducing the natural gas consumption on the short term.

The paper presents the heat pump design and evaluation results within the HP-Launch (High Performance Little Air Unit Natural Charge Heatpump) project. The overall project objective was to develop a novel natural refrigerant based air to water heat pump that will accelerate the introduction of air source heat pumps to the Dutch market. Targeting at implementation in existing single family terraced houses, which represents approximately 45% of the installed base (Friedel, 2020). These houses are characterized by the limited space available for placement of a heat pump and typically the natural gas boiler is located at the attic.

The use of R-290 has become the main solution for using a natural refrigerant inside domestic heat pumps. R-290 is highly flammable (A3-class refrigerant). Therefore, refrigerant charge is a critical design parameter, especially for indoor placement where charge quantity is limited by safety regulations. The main goal of the heat pump design was validating feasibility of a low charge R-290 based air source heat pump in hybrid configuration with a natural gas boiler, by comparing the measured performance and efficiency with a state of the art commercially available hybrid heat pump.

In the following sections first the design specification of the heat pump is presented. Hereafter in Section 3 the performance calculation model used for component selection is discussed, followed by the initial component selection in Section 4. Section 5 discusses the charge calculation model, and section 6 presents the results of the charge measurement based on the PVT-superheat method, here also a comparison with the charge calculations is made, and using the validated charge model, the final components are selected.

The final prototype is presented in Section 7, and the results of the performance measurements of the prototype including a comparison with a reference heat pump are given in Section 8. Finally, the conclusion is presented in Section 9.

2. SYSTEM SPECIFICATIONS

Market survey (Friedel, 2020) performed as a task within the HP-Launch project, including interviewing various stakeholders, resulted in the following main requirements for the heat pump design:

- Installation near existing boilers in the attic using a "through the roof" design in which the system is completely installed from the inside of the house,
- Monoblock system, reducing requirements on qualification of installers,
- Nominal heating capacity of 3 to 3.5 kW at A7/W35 (EN14511),
- Energy efficiency comparable to best-in-class appliances on the market,
- Suitable for hybrid as well as full electric heating operation,
- Total system weight as low as possible, preferably below 20 kg,
- Use a natural refrigerant and apply a small charge,
- When using a hydrocarbon as the refrigerant, comply with the safety design limit of 150 grams for indoor units (EN-378, IEC 60335-2-40:2018),
- Use commercially available mass-produced components,
- Hot gas defrosting.

3. PERFORMANCE CALCULATION

For heat pump design and component selection a refrigeration cycle calculation model (Van Gorp, 2020) is set-up in Microsoft Excel 2016 combined with visual basic coding. The model is a time-independent calculation of the refrigerant state throughout the system and uses the refrigerant property data Refprop 10.0 (Lemmon et al, 2018) for the determination of the refrigerant properties. The model calculates the performance of the individual components (i.e., compressor, condenser, evaporator, and the internal heat exchanger), which is then combined into a heat pump cycle model. Iterative calculations are used to update the condensing and evaporating pressure to reach agreement between the different sub models describing the components. These sub models, tuned using measurement and manufacturer data, are outside the scope of this paper.

The superheat is directly controlled by an electronic expansion valve. Therefore, the setpoint of this control is used as the input parameter for the model. The subcooling depends (amongst others) on the amount of refrigerant inside the system. With a fixed superheat at the evaporator outlet, excess refrigerant will accumulate inside the condenser as liquid. Since the objective of the project is to have a low refrigerant quantity inside the system, a low amount of subcooling (2 K) is assumed in the calculations.

The inputs of the cycle model are the outdoor air temperature and humidity, the water inlet temperature and flow rate, and the speed of the compressor and fan. The main output of the model is the heating capacity and the input power of the compressor and the fan.

4. INITIAL COMPONENT SELECTION

4.1. Compressor

Although increasing, availability of R-290 compressors models was limited at the time (2018) of component selection. Searching for suitable R-290 compressors, based on swept volume, isentropic efficiency and weight resulted in the options presented in Table 1. The nominal heating capacity, calculated using the cycle model, is based on an evaporating temperature of 2 °C, a condensing temperature of 36 °C, a refrigerant subcooling of 2 K and a superheating of 10 K and the compressor efficiencies and swept volume presented in Table 1. Based on weight (i.e., volume), and controllability, compressor options 4 and 5 were selected.

Table 1: Compressor options. (Except for heating capacity, the values are based on the manufacture data)

Option	Type	Displacement	Speed [rpm]	Nominal heating capacity [kW]	Isentropic efficiency [-]	Volumetric efficiency [-]	Weight [kg]
1	Rotary	24.4 cm ³	≈3000	4.0	0.59	0.82	14
2	Rotary	22.3 cm ³	≈3000	3.8	0.67	0.88	14.6
3	Rotary	18.4 cm ³	≈3000	3.1	0.69	0.86	13.8
4	Rotary	17.9 cm ³	600 to 7200	3.7	0.67	0.90	9.7
5	Rotary (Twin cylinder)	18.1 cm ³	480 to 7200	3.8	0.68	0.90	8.5
6	Scroll	5.8 m ³ h ⁻¹	≈3000	5.5	0.63	-	23

4.2. Condenser

Plate type heat exchangers are the standard solution for domestic air to water heat pumps. Therefore, condenser selection is based on selecting a plate heat exchanger showing lowest refrigerant volume for acceptable performance. Based on manufacturer data an asymmetric plate heat exchanger with a refrigerant volume of 0.0204 dm³ per channel was selected. Using manufacturer selection software (SWEP SSP8) heat exchanger performance was calculated for the number of plates used, based on a heat rejection of 4 kW, a refrigerant inlet temperature of 70 °C, a subcooling temperature of 3 K and a water inlet and outlet temperature of respectively, 30 and 35 °C. The result of these calculations are presented in Table 2.

Table 2: Calculation results of the selected condenser applying various plate numbers

Number of plates [#]	Refrigerant volume [dm ³]	HEX Mass [kg]	Heating capacity [kW]	Refrigerant inlet temperature [°C]	Water inlet temperature [°C]	Water outlet temperature [°C]	Subcooling [K]	Condensing temperature [°C]	ΔT refrigerant (pressure losses) [K]	Net pumping power [W]	Estimated pumping power (pump efficiency 25%) [W]
42	0.408	3.32	4	70	30	35	3	34.6	0.26	1.4	5.6
40	0.388	3.20	4	70	30	35	3	34.6	0.28	1.5	6.1
35	0.347	2.96	4	70	30	35	3	34.8	0.33	1.8	7.4
30	0.286	2.61	4	70	30	35	3	35.1	0.46	2.5	10.1
28	0.265	2.49	4	70	30	35	3	35.2	0.52	2.9	11.4
22	0.204	2.14	4	70	30	35	3	35.8	0.79	4.4	17.5
16	0.143	1.78	4	70	30	35	3	37.0	1.38	7.8	31.2

Table 2 shows that with 28 plates the calculated condensing temperature approaches the water outlet temperature and that only marginal reduction in condensing temperature results for increasing the number of plates above 40. The calculation indicates that required pumping power strongly increases below 28 plates. Based on availability, condensers samples with 30 and 40 plates were evaluated in the project.

4.3. Evaporator

Evaporator design is based on efficiency, low refrigerant charge, low noise, and proper defrosting and water removal. It was a dedicated activity in the HP-Launch project, which is outside the scope of this paper. The design activities (Doornbos, 2020), resulted in an evaporator with the following characteristics:

- Size: 800 x 360 x 52 mm (Height, Width, Depth)
- Tubing: 3 rows in depth, 40 rows in height, with 10 parallel circuits, and 5 mm tubing
- Fin pitch: 1.8 mm
- Fans: two, 5 bladed, EC fans with a diameter of 350 mm

The actual built of a prototype evaporator was outside the scope of the project. Based on good agreement in tube diameter, fin pitch and overall surface area, two commercially available mini channels heat exchangers were bought. Namely, one sample with 2-tubes in airflow direction and a second sample with 3-tubes in airflow direction, see Table 3 where the characteristics of the selected evaporators are presented.

Table 3: Evaporator characteristics. (The UA values are calculated with the performance model at the presented temperatures and air flow)

Tubes in depth [no#]	Tubes in height [no#]	Tube diameter [mm]	Fin pitch [mm]	Height (fin package) [mm]	Width (fin package) [mm]	Depth (fin package) [mm]	Refrigerant volume [dm ³]	HEX total Mass [kg]	UA value [WK ⁻¹]	Evaporating temperature [°C]	Air inlet temperature [°C]	Airflow [m ³ h ⁻¹]
3	24	5	1.8	480	695	52	1.2	27	641	6.3	7.0	1928
2	24	5	1.8	480	695	38.5	0.9	25	445	6.3	7.0	1928

4.4. Other refrigeration components and tubing

A refrigerant distributor, with 9 connections was designed and manufactured. To minimise system refrigerant content, the distributor was installed as close as possible to the expansion valve. Capillary tubing with a length of 1.2 m and an inner diameter of 1.8 mm was used to connect the distributor to the evaporator. The reversing valve and two-way expansion valve were selected based on direct availability, only. The suction gas heat exchanger, included to increase system efficiency (4.6% increase in COP at A7/W35, calculated with the performance model), has a liquid volume of 8.3 cm³ and a vapour volume of 23 cm³ and was selected based on small internal volume and direct commercial availability. To obtain minimum refrigerant volume, the filters (Vulkan Lokring, model DR10), installed at both sides of the expansion valve, were modified. The original filters were cut, the absorbent was removed, and a standard pipe reducer coupling (5/8" to 1/4") was fitted directly after the internal filter-gauze resulting in a filter with an internal volume of 6.9 cm³, see Figure 1 where a picture of the filter is shown.



Figure 1: Home-made filter. The picture is of a first trial in which a similar filter with a reduced outlet was modified. In the prototype the filters are of equal overall dimensions but are made by modifying the Vulkan Lokring DR10 filter/drier depicted above.

To reduce the risk of rupture, the discharge and suction tubing are installed with additional flexibility. To minimise the required system refrigerant charge, the other tube connections are made as short as possible, with special attention for the liquid line volume. The final tube dimensions are presented in Table 4.

Table 4: Tube dimensions

	Material	Outer diameter [mm]	Wall thickness [mm]	Total tube length [m]
Discharge line	Copper	6.35 (1/4")	0.8 mm	1.25
Liquid line	Copper	6.35 (1/4")	0.8 mm	0.23
Suction line	Copper	9.52 (3/8")	0.8 mm	2.20

5. CHARGE CALCULATION MODEL

A numerical model, originally developed for estimating the refrigerant charge of commercial refrigeration appliances (Van Beek en Van Gorp, 2018) was used to estimate the difference in refrigerant charge for the component options. The model has been set up in Matlab 2018 using the refrigerant property data Refprop 10.0 (Lemmon *et al*, 2018). Using Eq. (1) the model estimates the total refrigerant charge of the heat pump for stationary operation at a specific operating condition. In the model the system is split up in the following sections (i.e., components): discharge line, condenser, liquid line, filter, evaporator, suction tube, compressor shell and the lubricant oil. Component dimensions, heat transfer values and appliance operating conditions (i.e., system pressures and temperatures) are input parameters and are expected to be known from system design. Except for the condenser, evaporator, filter and the lubricant, the refrigerant mass is derived using Eq. (2), where refrigerant density is derived from the pressure and temperature using Refprop 10.0.

$$M = \sum_{i=1}^n a_i V_i + a_{oil} M_{oil} \quad \text{Eq. (1)}$$

$$m_i = \rho_i V_i \quad \text{Eq. (2)}$$

The model assumes that two-phase flow can only exist within the condenser, evaporator, and the filter. The condenser and the evaporator are split into two-phase and single-phase regions, and it is assumed that each parallel circuit of the heat exchanger shows the same behaviour, with equally divided refrigerant charge. Therefore, the total component refrigerant mass results after multiplying the charge calculated for a single circuit with the total number of parallel circuits. For the two-phases regions calculations are performed applying various void fraction correlations, (22 in total). These correlations, including both slip ratio correlations and drift flux correlations were selected from available literature, see section 5.2 where a brief summary of this research is presented.

For the condenser and the evaporator, the length of the two-phase flow region is calculated by subtracting the length of the subcooled and superheated region from the total length of the heat exchanger. The length of these single-phase regions is calculated using 50 calculation elements of equal temperature step (i.e. prescribed refrigerant temperature change and hence refrigerant heat transfer). For each element (k) the corresponding length (L_k) is calculated from the heat absorption / rejection, the overall heat transfer value of the element (UA_k) and the temperature difference between the refrigerant and the air following Eq. (3). UA_k of the element (subcooled or superheated) is estimated assuming a constant thermal resistance between the air and the outer surface of the heat exchanger and between the tube wall and the outer surface, and applying 1-D heat transfer theory. In such case the only difference in thermal resistance between the various sections of the heat exchanger (i.e. subcooled, two-phase, superheated) results from the differences in the refrigerant side heat transfer coefficient (h_r), and UA_k can be derived from the known overall heat transfer value based on two-phase flow (UA_{HEX}) following Eq. (5) to Eq. (7). The heat transfer coefficients (h_r) are estimated using the correlations of Gungor and Winterton (1987), for evaporating sections, the correlations of Mathur (1998), for condensing sections and using Janna (2000), for single-phase flow. For each element the refrigerant mass is calculated from the density and the volume and total mass is derived from summation over all elements.

$$L_k = \frac{1}{Q_k} \frac{\Delta T_{a-r,k}}{h_{r,k} P_k + \frac{\text{Const}}{L_{HEX}}} \quad \text{Eq. (3)}$$

With,

$$Q_k = UA_k \Delta T_{a-r,k} = \dot{m} \Delta h_{r,k} \quad \text{Eq. (4)}$$

$$UA_K = \frac{1}{\frac{1}{h_{r,k}P_KL_k} + \frac{Const}{L_{HEX}}L_k} \quad \text{Eq. (5)}$$

$$Const = \frac{1 - UA_{HEX}R_{(e,c)}}{UA_{HEX}} \quad \text{Eq. (6)}$$

$$R_{(e,c)} = \frac{1}{h_{(e,c)}P_{HEX}L_{HEX}} \quad \text{Eq. (7)}$$

The two-phase flow regions of the heat exchangers are divided into 100 calculation elements of equal length. The calculations are based on conservation of mass and assuming uniform heat flux, constant pressure, and equilibrium between the phases. Based on this, the mass of condensing or evaporating refrigerant is equal for each element. For each element, the local vapor quality is determined, and the slip ratio is calculated using one of the 22 correlations, hereafter the void fraction is calculated using Eq. (8). Note: Drift flux correlations were converted into a slip ratio correlation format.

$$\alpha_k = \frac{1}{1 + \frac{1 - x_k}{x_k} \frac{\rho_v}{\rho_l} S_k} \quad \text{Eq. (8)}$$

Finally, the total refrigerant mass within the two-phase section is calculated using Eq. (9).

$$M_{(e,c)} = \sum_{k=1}^n [(\alpha_k \rho_v + (1 - \alpha_k) \rho_l) V_k] \quad \text{Eq. (9)}$$

For the filter, the refrigerant mass is calculated using Eq. (10), where void fraction α_f needs to be between 0 (completely liquid) and 1 (completely vapor).

$$m_f = [\alpha_f \rho_v + (1 - \alpha_f) \rho_l] V_f \quad \text{Eq. (10)}$$

The mass of refrigerant dissolved in the lubricant oil is derived using equation (11) applying solubility data of R-290 (Polyolester SEZ 68 with R-290, (Bock and Puhl, 2010)), assuming that all lubricant oil is located inside the compressor shell being at discharge pressure and shell temperature.

$$m_{oil} = a_{oil} M_{oil} \quad \text{Eq. (11)}$$

5.1. Background in the selection of the void fraction correlations

Kuijpers et al. (1987) showed, by experimental validation of small heat exchangers (i.e. domestic appliances), that both the Premoli and the Hughmark correlation show acceptable agreement when calculating the refrigerant charge in evaporators. They concluded that for calculation of the mean void fraction in both condensing and evaporating flow the Premoli correlation can be considered to be superior. F. Poggi et al. (2008) concluded that some of the most used correlations, depending on mass flux, are Hughmark, Premoli and Tandon. Woldesemayat (2006) presented a detailed comparison of void fraction correlations for two-phase flow in horizontal and upward inclined flows in his Master thesis report. The work, based on more than 80 void fraction correlations, showed that best agreement results for the Toshiba, Rouhani-Axelsson, Dix, Premoli, Hughmark and Filimonov correlations. Jin and Hrnjak (2016) developed and validated a semi-empirical model to predict the refrigerant and lubricant quantity in both a microchannel condenser and a plate-and-fin evaporator for an air conditioning system. They evaluated six void fraction correlations for the condenser; Zivi, homogeneous, Premoli, Niño, Hughmark and a Zivi correlation modified for the effect of the oil. For the evaporator they evaluated four void fraction correlations, namely Zivi, Mandrusiak and Carey, Jassim and the homogeneous model. Their validation showed best agreement with the actual refrigerant charge for the Hughmark correlation in the evaporator and for the Jassim correlation in the condenser. The correlations mentioned above are included in the analyses. Next to this several other correlations, taken from Woldesemayat (2006) are included.

6. CHARGE MEASUREMENT AND FINAL COMPONENT SELECTION

For the selected compressor (single and twin cylinder) and condenser (30 or 40 plates) options charge measurements were performed using the PVT-superheat method. For this a heat pump was constructed in which fast closing valves (pneumatic controlled ball valves) were installed. Note: This heat pump does not include the selected evaporator, filter, and tubing. As shown in Figure 2 the valves divide the system in 5 control volumes (CV1 to CV5) and each volume is connected to the measurement vessel. The heat pump was operated at steady state with ambient air of 7 °C, a water inlet temperature of 35 °C, fixed water flow rate of 8.6 kg(min)⁻¹, 10 K superheat, a compressor speed of 3600 rpm, and an airflow of 1930 m³h⁻¹. After optimising the refrigerant charge toward maximum COP, the valves were closed, and the refrigerant charge was measured (U(M) = ± 1 g). Table 5 shows a 26.5 g lower refrigerant charge for using the 30-plate condenser compared to the 40-plate condenser and a 5 g lower refrigerant charge for using the twin cylinder compressors compared to the single cylinder compressor. Note: The shell of the twin cylinder (D = 107 mm, H = 254 mm) is smaller than the shell of the single cylinder compressor (D = 116 mm, H = 261 mm). The larger measured volume of the twin cylinder therefore completely results from the much larger suction muffler of this compressor. For both compressors the shell is at discharge pressure.

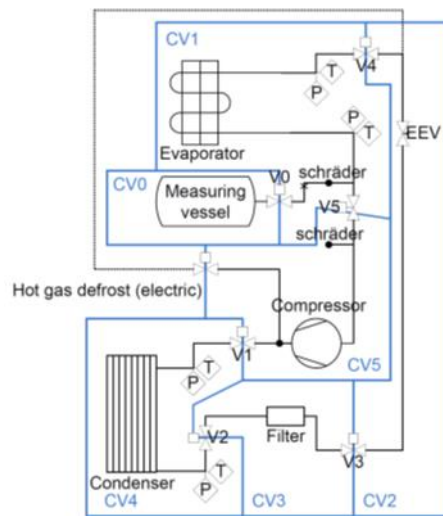


Figure 2: Principle sketch of the prototype heat pump used for charge measurement with PVT-superheat method.

Table 5: Measured control volume and refrigerant charge

	Control volume	Internal volume [ml]	Charge R-290 [g]
CV5	Compressor + oil (single cylinder)	1660	51.0
CV5	Compressor + oil (twin cylinder)	1915	46.0
CV4	Condenser 40 plates	440	73.5
CV4	Condenser 30 plates	324	47.0
CV0	Total system with 40-plate condenser and single cylinder compressor	2854	170.0
CV0	Total system with 30-plate condenser and twin cylinder compressor	2980	136.0

6.1. Model validation and void fraction correlation selection

Using the numerical model, applying all 22 void fraction correlations, the refrigerant charge was calculated and compared with the charge measurements. The calculations showed best agreement with the measurements for using the Armand-Massina (Arm-Mas) correlation for the evaporator and using the Hughmark (Hugh) correlation for the condenser, see Figure 3 and Table 6.

The Arm-Mas correlation is based on the homogeneous model and includes a linear correction factor in terms of the vapour quality. It does not include dependency of other dimensionless quantities such as, Reynolds, Froude or Weber number. The Hughmark correlation corrects the homogeneous model based on the

Reynolds number, the Froude number, and a no slip liquid volume fraction to adapt it to work in both horizontal and vertical orientations. As the Reynolds number depends on the void fraction, the Hughmark correlation needs to be calculated iteratively. Woldesemayat (2006) concludes from extensive comparison that the Arms-Mas and Hughmark correlations are applicable for both horizontal and vertical flows. Both these models have mainly been developed for air-water flows inside tubes. The limited validation performed in this study indicates that the models translate reasonably well to R290 refrigerant and the use of plate heat exchangers. This, however, requires further investigation.

To improve the agreement of the calculation model of the overall design with the measured refrigerant mass, the calculations are corrected by applying a 20 K warmer shell temperature than measured, and a 50% void fraction for the filter. The unexpected tuning of the void fraction for the filter needs further evaluation.

Table 6: Measured and calculated refrigerant mass for Configuration A: Single cylinder compressor and 40-plate condenser, and for Configuration B: Twin cylinder compressor and 30-plate condenser.

Control volume	Configuration A			Configuration B		
	Meas. [g]	Calc. [g]	Diff. [g]	Meas. [g]	Calc. [g]	Diff. [g]
Compressor	51.0	58.2	7.2	46.0	51.9	5.9
Condenser	73.5	77.3	3.8	47.0	50.1	3.1
Filter	8.8	7.6	-1.2	9.0	7.6	-1.4
Expansion valve + liq. line	7.6	8.2	0.6	8.0	8.2	0.2
Evaporator	25.4	26.2	0.8	26.0	26.4	0.4
Total system	170.0	177.5	7.5	136.0	144.2	8.2

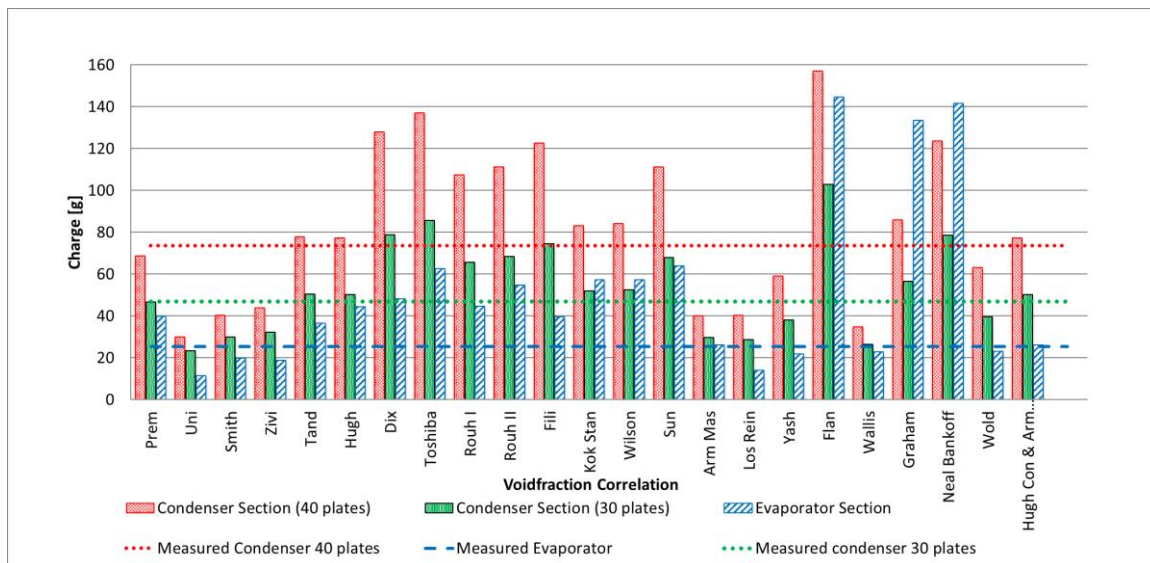


Figure 3: Charge calculation results for the evaporator and condenser sections based on the 22 evaluated correlations.

6.2. Final component selection based on calculated refrigerant charge

Table 7 shows the results of calculating total system refrigerant charge, heat pump performance, and COP based on the twin cylinder compressor and the selected heat exchanger options. Based on its lower measured refrigerant charge, lower weight, and higher efficiency the twin cylinder compressor was selected for the prototype. The table shows that an estimated charge of close to 150 g only results for combining the 2-row evaporator with the 30-plate condenser. Therefore, this configuration is selected for the prototype. The table also shows that this configuration has a 9.5% lower calculated heating capacity, a 9.5% lower COP, and a 4.2% lower SCOP than the best performing configuration, based on using the 3-row evaporator and the 40-plate condenser.

Table 7: Calculated refrigerant charge, heating performance, and COP for various heat exchanger options. Heating capacity and COP calculated at EN14511 A7/W30, with a compressor speed of 3600 rpm and airflow of 1930 m³h⁻¹. SCOP calculated based on the part-load conditions resulting from the reference house (Section 8).

		3-row evaporator and 30-plate condenser	2-row evaporator and 30-plate condenser	3-row evaporator and 40-plate condenser	2-row evaporator and 40-plate condenser
Compressor shell (twin cylinder)	[g]	36.4	36.3	36.3	36.3
Oil	[g]	21.6	21.6	21.6	21.6
Discharge tubing	[g]	0.5	0.5	0.5	0.5
Condenser	[g]	57.2	57.1	80.4	80.3
Liquid line	[g]	1.9	1.9	1.9	1.9
Filter (calculation based on subcooled liquid ($\alpha_f = 0$))	[g]	3.3	3.3	3.3	3.3
Expansion valve to distributor	[g]	0.6	0.6	0.6	0.6
Evaporator	[g]	41.5	26.4	48.7	31.5
Suction tube	[g]	0.9	0.9	0.9	0.9
Suction gas heat exchanger	[g]	4.2	4.2	4.2	4.2
Total system	[g]	168.1	152.8	198.4	181.1
Calculated heating capacity	[kW]	3.69	3.35	3.70	3.36
Calculated COP (A7/W35)	[-]	4.77	4.39	4.85	4.45
Calculated SCOP	[-]	4.03	3.90	4.07	3.93

7. PROTOTYPE HEAT PUMP

Figure 4 shows a picture of the prototype heat pump, which consists out of an 18.1 cm³ twin cylinder rotary compressor (GMC DSM180D19UDZ), a refrigerant to air heat exchanger having refrigerant tubing with a diameter of 5 mm and two rows in depth (LU-VE LMC3N 1510). The evaporator is connected to the expansion valve through 9 parallel circuits using a homemade distributor. The system has a 30-plate condenser with asymmetric plate distance (SWEP B8LAS), a reversing valve (Danfoss STF0101G), an internal heat exchanger to increase system efficiency (Danfoss HE05), two filters (homemade), and an electronic expansion valve (Carell E2V14BSF00). The refrigerant tubing is as presented in Table 4, and a single EC fan with a diameter of 350 mm is applied (Papst model: A3G350-AN01-11).

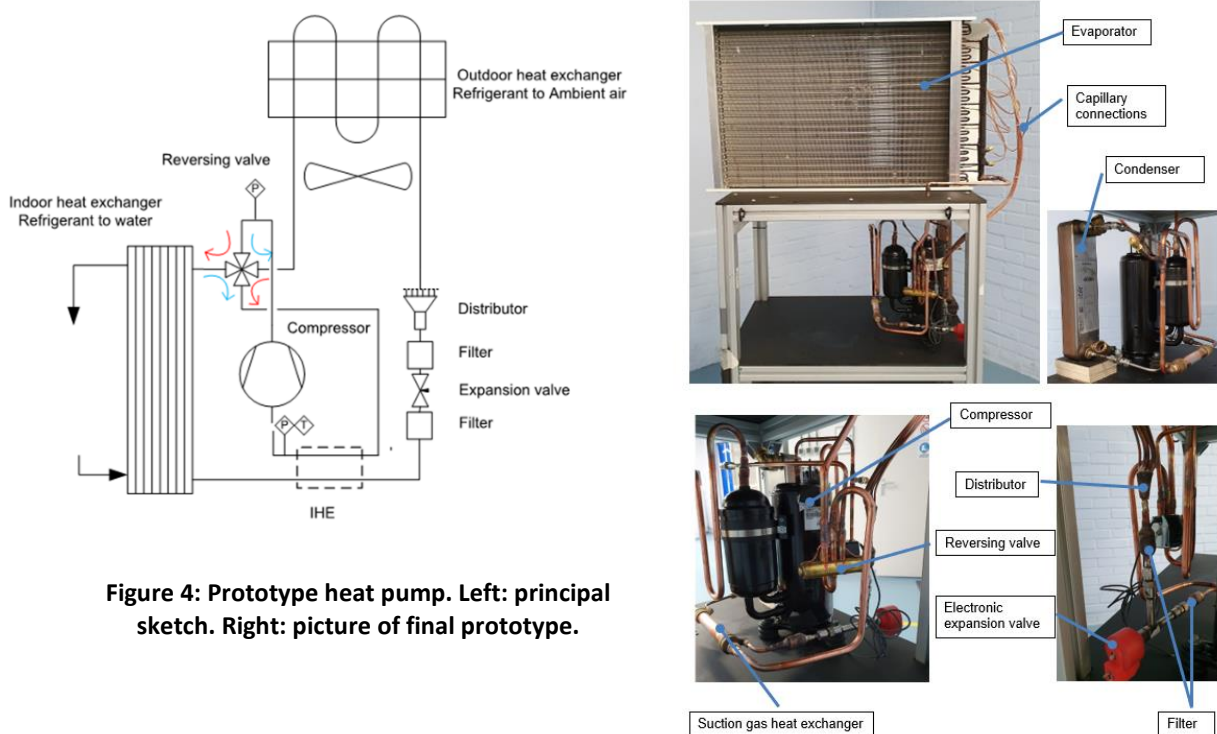


Figure 4: Prototype heat pump. Left: principal sketch. Right: picture of final prototype.

8. PERFORMANCE MEASUREMENT

8.1. Test set-up

The overall performance of the heat pump is measured using a climate chamber and a controlled water loop in line with EN 14511, except for uncertainty in measured temperature. Refrigerant temperatures are measured ($U(T) = \pm 0.3 \text{ }^\circ\text{C}$) with type T thermocouples using a Fluke Helios 1 data acquisition system, pressure transducers (Keller PA33X) are used to measure the refrigerant pressure ($U(P) = \pm 0.2\%$) at the compressor discharge, evaporator outlet, and the suction tube. System input power is measured ($U(P) = \pm 0.5\%$) using a power analyser (Yokogawa WT1600). The condenser water inlet and outlet temperature are measured using PT100 elements ($U(T) = \pm 0.2 \text{ }^\circ\text{C}$), and a Coriolis mass flow meter (Micromotion CMF050) is used to measure the water flow ($U(\dot{m}) = \pm 0.25\%$ reading). The air inlet temperature of the evaporator is measured using a grid of thermocouples (8 positions) ($U(T) = \pm 0.3 \text{ K}$) and a resistive electrolytic Humidity Probe (Novasina nSens-HT-ENS) was used to measure air humidity ($U(\text{Rh}) = \pm 1.5\% \text{ Rh}$) at the evaporator inlet.

Compressor speed was not controlled, and a fixed compressor speed was applied for each specific test. Defrosting was performed manually, by switching the compressor, reversing valve and the evaporator fan. Superheat is measured from the temperature measurement on the suction line and the saturation temperature calculated from the measured suction pressure using Refprop 10.0 (Lemmon et al, 2018). The superheat is controlled by the expansion valve using computer control with a LabVIEW based PID controller. Experimental validation showed highest system COP for controlling the superheating at the evaporator outlet at 5 K.

8.2. Test results

The prototype heat pump is measured on performance and efficiency. For comparison also a reference unit was measured. The reference unit was selected based on: commercial availability in the Dutch market, hybrid operation, a capacity range which is close to the design capacity of the 3.5 kW defined for the HP-Launch project, and efficiency of A++ level (low temperature). Which is the second-best efficiency class for heat pumps following Commission Delegated Regulation (EU) No 811/2013. This resulted in the selection of a Hybrid heat pump, which uses 1.4 kg of R-410A as the refrigerant and has a rated heating capacity of 3 kW and a COP of 4.8 at the EN 14511 reference condition A7 / W35.

Table 8 shows that at the EN 14511 reference condition A7 / W35 and a refrigerant charge of 150 gram, the COP of the prototype is measured at 4.47 and the heating capacity is measured at 3.4 kW. This is close to the design capacity of 3.5 kW. Testing at the optimum refrigerant charge (charge resulting in maximum COP) of 170 gram showed that the heating capacity and COP can be increased to $Q = 3.5 \text{ kW}$ and $\text{COP} = 4.63$. This COP is almost identical to the reference unit, for which a COP of 4.67 is measured at the EN 14511 reference condition. The reference unit shows a measured heating capacity of 4.7 kW, which is much larger than the rated capacity of 3 kW.

Heat pump performance is measured at part-load conditions for medium and low temperature application for the reference heating season “average” following EN 14825. The part load heating capacity was determined from the heat load curve resulting from the reference house selected within the HP Launch project (Friedel, 2020). This is a linear heat load curve from 5.5 kW, at an outdoor temperature of $-10 \text{ }^\circ\text{C}$, to 0 kW at an outdoor temperature of $+15 \text{ }^\circ\text{C}$.

To compare the two heat pumps, the Seasonal space heating energy efficiency (η_s) and energy label are calculated following (EU) No 811/2013 for a low and medium temperature application at the reference heating season “average”. The calculations are based on a hybrid package existing out of the heat pump (measured values) combined with a hypothetical A-label gas fired boiler ($\eta_{s,BU} = 94\%$) with a heating capacity to match the load curve of the reference house. Table 9 shows an identical η_s for the HP-launch and the reference system for operation in a medium temperature application.

For a low temperature application, the reference package, having an A+++ label, is however more efficient than the package based on the HP Launch prototype which reaches A++ efficiency. The table also shows, as expected, that due to the higher heating capacity, the reference heat pump covers a larger portion of the heating demand.

Table 8: measurement results at the EN 14511 reference condition A7 / W35, using a compressor speed of 3600 rpm and an airflow of 1930 m³h⁻¹ for the prototype.

Measured performance	Prototype 150 g R-290	Prototype 170 g R-290	Reference system
Heating capacity	3414 ± 121 W	3511 ± 121 W	4697 ± 189 W
Input power Compressor	692.4 ± 3.5 W	691.4 ± 3.5 W	
Input power Fan	53.2 W	47.7 W	
Mass flow water	8.6 ± 0.02 kg(min) ⁻¹	8.6 ± 0.02 kg(min) ⁻¹	13.5 ± 0.03 kg(min) ⁻¹
Pressure difference water	0.11 bar	0.10 bar	0.01 bar
Input power circulation pump (calculated following EN 14511)	18.8 W	18.4 W	-4.9 W
Total input power	764.4 ± 3.8 W	757.6 ± 3.8 W	1010 ± 5.1 W
COP	4.47 ± 0.16	4.63 ± 0.16	4.65 ± 0.19

Table 9: Calculated seasonal space heating energy efficiency following (EU) No 811/2013, without hot water storage tank and with a class II temperature controller, for low (LT) and medium temperature (MT) application at the reference heating season “average”, and the heating demand of the reference house.

Heat pump	Boiler ($\eta_{s,BU} = 94\%$)	Heating by heat pump	LT η_s (label)	MT η_s (label)
Reference	2.5 kW	98%	180% (A+++)	135% (A++)
HP Launch	4.0 kW	85%	157% (A++)	135% (A++)

9. CONCLUSIONS AND DISCUSSIONS

The project showed that an air to water heat pump with a heating capacity of 3.5 kW and a COP of 4.5 (A7/W35, EN 14511) can be designed and built for a maximum R-290 refrigerant charge of 150 g using commercially available components. Laboratory measurements show that if applied in a typical Dutch house, based on seasonal space heating energy efficiency, the heat pump can compete with current state of the art heat pump systems.

It is shown that the charge model developed can assist in the design of low charge heat pump systems. The calculations and measurements show that efficiency improvements of up to 9.5% on COP can be obtained when accepting an increase in refrigerant charge from 150 to 200 g.

Heat pump design standards are changing into the direction of allowing larger refrigerant charges of R-290. However, regarding safety it remains preferred to design for the lowest possible R-290 charge meeting the performance and efficiency requirements, especially for indoor installations.

The charge model shows good agreement with the measurements. However, only a very limited number of designs are experimentally validated. Therefore, further experimental validation of the model is recommended before using it for other heat pump designs.

NOMENCLATURE

a	average density	(kg m ⁻³)	Q	heat flow	(W)
a_{oil}	solubility of refrigerant in lubricant oil	(kg kg ⁻¹)	Q_H	Heating capacity	(W)
COP	Coefficient of performance	(-)	R	thermal resistance	(K W ⁻¹)

CV	Control volume	(m^3)	S	slip ratio	(-)
			$SCOP$	Seasonal heating performance	(-)
D	Diameter	(m)	T	temperature	($^{\circ}C$)
H	Height	(m)	UA	overall heat transfer rate	($W K^{-1}$)
h	heat transfer coefficient	($W m^{-2} K^{-1}$)	U	Expanded uncertainty, 95% confidence interval	(.)
L	length	(m)	V	volume	(m^3)
M	total refrigerant mass	(kg)	x	vapor quality	($kg kg^{-1}$)
M_{oil}	mass of lubricant oil	(kg)	α	void fraction	(-)
m	refrigerant mass	(kg)	Δh	specific enthalpy change	($J kg^{-1}$)
\dot{m}	mass flow	($kg s^{-1}$)	ΔT	temperature difference	(K)
P	Tube / channel perimeter	(m)	ρ	refrigerant density	($kg m^{-3}$)
P	pressure	(Pa)	η_s	Seasonal space heating efficiency	(-)
P	Power	(W)			
Subscript					
a	air side		k	calculation element index	
c	condensing / condenser		l	liquid	
e	evaporating / evaporator		oil	lubricant oil	
f	filter / drier		r	refrigerant side	
HEX	heat exchanger		v	vapor	
i	control volume index				

REFERENCES

- Beek, M. van, Gorp, T. van, 2018. Charge Equation For Low Charge Based Commercial Refrigeration Appliances. Proceedings of the 17th International Refrigeration and Air Conditioning Conference, paper 2618
- Bock, W., Puhl, C. (2010), *Kältemaschinenöle*, Berlin: VDE Verlag GMBH.
- Doornbos, G. J., 2020, "Ontwerp verdampersysteem", HP Launch – Workpackage 2
- De Rossi, F., Mauro A.W., Musto M., Vanoli G.P. (2011), Long-period food storage household vertical freezer: Refrigerant charge influence on working conditions during steady operation, *Int. J. Refrig.* 34(5), 1305-1314.
- Friedel, P., 2020 "Randvoorwaarden voor systeemontwikkeling" HP Launch – Workpackage 1
- Gorp, T. van, 2020, "Performance calculation model", HP Launch – Workpackage 2
- Gungor, K.E., Winterton, R.H.S. (1987). Simplified general correlation for saturated flow boiling and comparison with data. *Chem Eng Res Des*, 65, 148–156
- Janna, S. W. (2000). *Engineering heat transfer, second edition* (page 324). Boca Raton, FL: CRC Press.
- Jin, S. and Hrnjak, P. (2016), Refrigerant and lubricant charge in air condition heat exchangers: Experimentally validated model, *International Journal of Refrigeration*, 67, 395-407
- Kuijpers, L., Janssen, M., de Wit, J., (1987), Experimental verification of liquid hold-up in small refrigeration heat exchangers, in *XVIIth International Congress of refrigeration, Vienna*, 307–315
- Lemmon, E.W., Bell I.H., Huber, M.L., McLinden, M.O. NIST Standard Reference Database 23: Reference Fluid Thermodynamic and Transport Properties-REFPROP, Version 10.0, National Institute of Standards and Technology, Standard Reference Data Program. Gaithersburg, 2018.
- Mathur, G.D. (1998), Heat transfer coefficients for propane (R-290), isobutene (R-600a), and 50/50 mixture of propane and isobutane, In *ASHRAE Transactions 104,2, ASHRAE Annual meeting, Atlanta, United States of America* (1159-1172)
- Poggi, F., Macchi-Tejeda, H., Leducq D., Bontemps A. (2008), Refrigerant charge in refrigerating systems and strategies of charge reduction, *International Journal of Refrigeration*, 31(3), 353-370.
- Premoli, A., Di Francesco, D., Prina, A., (1970), Una correlazione adimensionale per la determinazione della densità di miscele bifasiche, in *XXV Congressor Nazionale ATI, Trieste, Italy*, 120-129
- Woldesemayat, M. A. (2006). *Comparison of void fraction correlations for two-phase flow in horizontal and upward inclined flows* (Oklahoma State University).